

1

2

3 Comparison of enrichment methods for 4 efficient nitrogen fixation on a biocathode

5

6 Axel Rous¹, Gaëlle Santa-Catalina¹, Elie Desmond-Le Quémener¹, Eric
7 Trably¹, Nicolas Bernet¹

8

9 ¹ INRAE, Université de Montpellier, LBE, 102 avenue des Étangs, 11100 Narbonne, France

10

11 *Corresponding author

12 Correspondence: nicolas.bernet@inrae.fr

13

14

15 **ABSTRACT**

16 The production of nitrogen fertilizers in modern agriculture is mostly based on the Haber-
17 Bosch process, representing nearly 2% of the total energy consumed in the world. Low-
18 energy bioelectrochemical fixation of N₂ to microbial biomass was previously observed but
19 the mechanisms of microbial interactions in N₂-fixing electroactive biofilms are still poorly
20 understood. The present study aims to develop a method of enrichment of autotrophic and
21 diazotrophic bacteria from soil samples for further characterization. The enrichment
22 method was based on a first classical step of selection of N₂-fixing bacteria from soil
23 samples. Then, a polarized cathode was used for the enrichment of autotrophic bacteria
24 using H₂ (hydrogenotrophic) or the cathode as energy sources. This enrichment was
25 compared with an enrichment of diazotrophic hydrogenotrophic bacteria without the use of
26 the microbial electrochemical system. Both methods showed comparable results for N₂
27 fixation rates at day 340 of the enrichment with an estimated average of approximately 0.2
28 mgN_{fixed}/L.d. Current densities up to -15 A/m² were observed in the polarized cathode
29 enrichments and a significant increase of the microbial biomass on the cathode was shown
30 between 132 and 214 days of enrichment. These results confirm the enrichment of
31 autotrophic, electrotrophic and diazotrophic bacteria in the polarized cathode enrichments.

32 Finally, the analysis of the enriched communities suggested that *Desulforamulus ruminis*
33 mediated microbial interactions between autotrophic anaerobic and heterotrophic aerobic
34 bacteria in polarized cathode enrichment. These interactions could play a key role in the
35 development of biomass in these systems and on N₂ fixation. Based on these findings, a
36 conceptual model on the functioning of mixed cultures N₂-fixing electroactive biofilms was
37 proposed.

38

39

40 **Keywords:** Nitrogen fixation, Microbial electrochemical system, Biomass electrostimulation,
41 Enrichment method

42

43

44

Introduction

46 Nitrogen is one of the essential elements for the growth of all living organisms, especially for cellular
47 protein synthesis. In modern agriculture, ammonia is often used as a nitrogen source for plants (Bagali,
48 2012; Burris & Roberts, 1993; Masclaux-Daubresse et al., 2010). This compound is produced at industrial
49 scale by the Haber-Bosch process which allows the reduction of N_2 to NH_3 at the expense of large
50 quantities of H_2 and energy (Kandemir et al., 2013; Martin et al., 2019). This process is associated with
51 significant CO_2 emissions, due to the source of H_2 obtained either by methane steam reforming or coal
52 gasification (Martin et al., 2019). Alternatives for green H_2 production, such as water electrolysis, are
53 therefore nowadays considered to feed the Haber-Bosch process that is also contributing to a high
54 energy demand of the process (Cherkasov et al., 2015). A more direct alternative is to reduce N_2 directly
55 on a cathode by chemical catalysts. However, these catalysts are not renewable and are currently not
56 sufficiently selective regarding the hydrogen evolution reaction at ambient conditions (Deng et al., 2018;
57 A. Liu et al., 2020).

58 Recently some authors proposed to use N_2 -fixing bacteria in association with electrochemical systems
59 for N_2 reduction at low energy cost (C. Liu et al., 2017; Rago et al., 2019). This idea was inspired by
60 previous observations of microbial CO_2 fixation on microbial cathodes in a process known as microbial
61 electrosynthesis (A. Liu et al., 2020; Logan et al., 2019). The microbial fixation of both N_2 and CO_2 with a
62 polarized cathode was demonstrated in two recent studies (C. Liu et al., 2017; Rago et al., 2019). First, Liu
63 et al. (2017) (C. Liu et al., 2017) demonstrated the growth of *Xanthobacter autotrophicus* in a hybrid
64 organic-inorganic electrochemical system in the absence of nitrogen sources other than N_2 . Then, Rago et
65 al. (2019) (Rago et al., 2019) demonstrated N_2 fixation through microbial electrosynthesis (MES) with a
66 mixed microbial community. This new type of process had the potential to produce biomass from N_2 and
67 CO_2 with only electricity as energy input that could be provided by small production units such as solar
68 panels (Rago et al., 2019). This biomass could then be used as a fertilizer with a low impact on the
69 environment (Chakraborty & Akhtar, 2021; Rago et al., 2019; y. Hafeez et al., 2006). Although the proof
70 of concept was made for this process, the microbial interactions supporting N_2 fixation in this microbial
71 electrochemical systems are still poorly understood. Different N_2 fixation scenarios are indeed possible,
72 such as: (i) fixation by a single population capable of fixing N_2 and CO_2 using the electrode as sole energy
73 source, (ii) fixation by heterotrophic diazotrophic bacteria that can utilize the organic carbon produced by
74 electro-autotrophic bacteria, (iii) fixation through an interaction between methanogenic archaea and
75 methanotrophs that could use CH_4 as an energy source for N_2 fixation and (iv) fixation through an
76 interaction mediated by direct interspecies electron transfer (DIET) between electro-autotrophic bacteria
77 and diazotrophic bacteria (Rago et al., 2019). A better understanding of these interactions is essential to
78 optimize N_2 fixation in microbial electrochemical system.

79 In nature, biological N_2 fixation is a key mechanism of the nitrogen cycle where atmospheric nitrogen
80 is uptaken by living organisms (Bagali, 2012). It is carried out by so-called diazotrophic bacteria
81 responsible for the transformation of N_2 into NH_3 (Kim & Rees, 1994). Some of these bacteria can be
82 found on the roots of plants where they are living in symbiosis (Burris & Roberts, 1993; Franche et al.,
83 2009). These microorganisms are able to fix N_2 from the air, making it assimilable in the form of NH_4^+ or
84 amino acids (L-glutamine, L-glutamate) which are further used in plants for protein or DNA synthesis
85 (Burris & Roberts, 1993). In exchange, the bacteria use the organic matter of root exudates produced by
86 the plants as carbon and energy sources. Among the diazotrophic bacteria, the genera *Frankia* and
87 *Rhizobium spp.* are often associated with leguminous plant roots (Burris & Roberts, 1993; Peoples &
88 Craswell, 1992). In contrast, other free-living N_2 -fixing bacteria such as *Azospirillum*, are able to fix N_2
89 without interacting with plants and can use organic or inorganic materials to produce their own energy
90 (Tilak et al., 1986).

91 The fixed N is then used for the synthesis of proteins and in particular for the synthesis of L-glutamate
92 and L-glutamine which are inhibitors of nitrogenase synthesis (Moreno-Vivián et al., 1989; Y. Zhang et al.,
93 2022). Interestingly, nitrogenases are not fully specific and are able to catalyze other reactions such as
94 the production of H_2 and the reduction of ethylene to acetylene which require less energy (Burgess &
95 Lowe, 1996). The latter reaction is used to indirectly measure N_2 fixation rate by the acetylene reduction
96 assay (ARA) (Bergersen, 1970; Soper et al., 2021). This measurement has particularly contributed to the

97 better understanding of the microbial mechanisms supporting N₂ fixation (Bergersen, 1970; Saiz et al.,
98 2019; Soper et al., 2021).

99 In order to better understand the microbial mechanisms supporting N₂ fixation in polarized cathode
100 enrichment, this work aims at developing an enrichment method of cathodic biofilms for direct fixation
101 of CO₂ and N₂. For this, soil samples were used as sources of N₂-fixing bacteria, and successive
102 enrichments in autotrophic bacteria in polarized cathode enrichment (PCE) were performed to select a
103 electroactive biofilm capable of fixing N and C with a cathode as sole energy source. The enriched biofilm
104 was compared with a classical enrichment of N₂-fixing hydrogen-oxidizing bacteria (HOB) in flasks (named
105 H₂ enrichment, H₂E) (X. Hu et al., 2020; C. Liu et al., 2017).

106 **Methods**

107 **Inoculum**

108 Soil samples from a forest, agricultural crop field and a commercial compost were used as microbial
109 inoculum sources. Samples were collected from forest and agricultural soils in the Haute Vallée de l'Aude,
110 France. These sources were selected based on their assumed abundance of N₂-fixing bacteria and their
111 theoretical C/N ratio (Khan et al., 2016). One to two mg of each samples were used as inoculum in 50mL
112 of medium for preliminary enrichment culture.

113 **Culture media**

114 The culture media were both formulated on the basis of H3 medium (81 DSMZ) used for enrichment
115 of soil autotrophic bacteria. The medium consisted of 2.3g KH₂PO₄ and 2.9g Na₂HPO₄ 2H₂O per liter as
116 buffer, 0.5g MgSO₄ 7H₂O, 0.01g CaCl₂ 2H₂O, 0.005g MnCl₂ 4H₂O, 0.005g NaVO₃ H₂O, and 5mL of SL-6
117 trace element solution per liter of medium, with 5mL of vitamin solution. The vitamin solution consisted
118 of 0.1g ZnSO₄ 7H₂O, 0.03g MnCl₂ 4H₂O, 0.3g H₃BO₃ 0.2 CoCl₂ 6H₂O, 0.01g CuCl₂ 2H₂O, 0.02g NiCl₂ 6H₂O,
119 and 0.03g Na₂MoO₄ 2H₂O per liter of solution. Iron citrate was added to the enrichment bottles at a
120 concentration of 0.05 g/L but not to the microbial bioelectrochemical systems in which the cathode was
121 used as sole electron source. An organic carbon solution (organic C) was composed of 2g/L D-glucose,
122 1g/L yeast extract, 1g/L Na-acetate, 1g/L DL-malic acid, 1g/L Na-lactate, 1g/L Na-pyruvate, and 1g/L D-
123 mannitol and used when indicated. NH₄Cl was added at 1 g/L only when indicated. All enrichment
124 procedures were maintained at 30°C and the pH was adjusted to 6.8 with NaHCO₃ in the microbial
125 bioelectrochemical systems and the enrichment cultures without organic C addition. When the organic C
126 solution was used, the pH was adjusted between 6.3 and 6.5.

127 **Design of microbial electrochemical system**

128 The electrochemical system used for our enrichment were composed of two chambers separated by
129 an anion exchange membrane (AEM) (fumasep[®] FAB-PK-130). The AEM was used to avoid the migration
130 of NH₄⁺ ions to the anodic chamber. Each chamber had a total volume of one liter. The pH of the reactors
131 was adjusted to 6.8 at the beginning of each batch experiment. Each system had a 25 cm² square carbon
132 felt working electrode with a thickness of 0.7 cm and a 16 cm² square Pt-Ir grid as a counter electrode.
133 The carbon felt electrodes were conditioned using chemical treatment with HCl, a flush with ethanol and
134 a heat treatment at +400°C as described elsewhere by Paul et al (Paul et al., 2018). The systems were
135 inoculated with the flask enrichments used for N₂ fixation in presence of organic C (N-free medium). After
136 inoculation, the organic C supply was reduced to 10% of the initial supply in all reactors. The organic C
137 supply was then totally replaced by CO₂ supply. Two of the systems were polarized and two other
138 reactors were used as controls with open current voltage (non-polarized cathode enrichment, nPCE). The
139 working electrodes of the polarized cathode enrichment (PCE) were poised at a potential of -0.940 V vs.
140 saturated calomel electrode (SCE) used as a reference. The system was connected to a VMP3.0
141 potentiostat (BioLogic). The current was measured over time by a chronoamperometry method and cyclic
142 voltammetry was performed every 3-7 days at the beginning of enrichment periods. The monitoring of
143 the current intensity was used to monitor the efficiency in enriching the biofilms in autotrophic and/or
144 electrorophic bacteria (Zaybak et al., 2013). The current density *J* was calculated using the surface of the
145 working electrode, i.e. 25 cm².

146 Before inoculation of the reactors, an initial chronoamperometry measurement was performed along
147 the first 2 days of operation with only organic carbon in the medium to determine the basal current
148 density in absence of bacteria. Two other abiotic reactors for 15 days were then implemented to
149 measure the current density in a medium without organic C.

150 The energy required for the production of microbial metabolites and for biomass growth was then
151 used to calculate the Coulombic efficiency of the PCE according to the equations 1-5:

152
153 Eq. 1 $2.1 H_2 + CO_2 + 0.2 NH_4^+ \rightarrow CH_{1.8}O_{0.5}N_{0.2} + 1.5 H_2O + 0.2 H^+$ for biomass production
154 ($21 \text{ mol}_e/\text{mol}_{\text{N}_{\text{biomass}}}$) (Wresta et al., 2021)

155
156 Eq. 2 $N_2 + 3 H_2 \rightarrow 2 NH_3$ for nitrogen fixation ($3 \text{ mol}_e/\text{mol}_{\text{N}_{\text{fixe}}}$) (L. Zhang et al., 2022)

157
158 Eq. 3 $2 CO_2 + 4 H_2 \rightarrow CH_3COO^- + H^+ + 2 H_2O$ for acetate production ($8 \text{ mol}_e/\text{mol}_{\text{CH}_3\text{COO}^-}$)
159 (Wresta et al., 2021)

160
161 Eq. 4 $2 H^+ + 2 e^- \rightarrow H_2$ for H_2 production ($2 \text{ mol}_e/\text{mol}_{\text{H}_2}$)

162
163 Eq. 5 $CE = \frac{n_e \times F \times n_{\text{product}}}{\int i dt}$

164 With CE the Coulombic efficiency in percentage of electron recovery in circuit, n_e moles of electrons
165 per moles of product ($\text{mol}_e/\text{mol}_{\text{product}}$) calculated from the stoichiometric equations, F the Faraday
166 constant ($96485 \text{ C} \cdot \text{mol}^{-1}$), n_{product} the number of $\text{mol}_{\text{product}}$ and i the current intensity.

167 **Enrichment procedures**

168 Two enrichment procedures based on a sequential procedure by enriching separately N_2 fixation and
169 the use of an inorganic energy source were carried out.

170 The first enrichment method was performed in three steps:

171 - The first step was performed in a 120 mL bottle with N-free medium supplemented with organic C
172 source. The headspace was composed of an O_2/N_2 mixture (10/90) at 0.5 bar (absolute pressure).
173 Cultures were carried out in bottles containing 50 mL of liquid and 70 mL of headspace. Subcultures of
174 these enrichments were performed every 7 days for 6 weeks. The time between 2 subcultures was then
175 reduced to 3-4 days using 10% of the volume of the previous culture (5mL/50mL).

176 - After 55 days of enrichment in 10 successive batches, the enriched cultures were used to inoculate
177 the cathodic chambers of the polarized microbial electrochemical system (Polarized Cathode Enrichment,
178 PCE) and the non-polarized microbial electrochemical system (non-Polarized Cathode Enrichment nPCE).
179 The same inorganic medium supplemented with 10% of the organic C source was fed each week to start
180 the enrichment of autotrophic bacteria. 80% of the medium was renewed every second week to promote
181 biofilm growth on the cathode. Headspace composition was monitored by GC and flushed with N_2 if pO_2
182 exceeded 10% of the gas volume. Organic C supply was stopped when a significant current density was
183 measured in the polarized systems with regard to the controls.

184 - In the third and final enrichment step, CO_2 was used as sole carbon source. A 80/20 (v:v) CO_2/N_2
185 atmosphere was set up in the headspace with trace amounts of O_2 (< 5%). The medium was replaced
186 every 15-30 days. The gas recycling vessel was filled with CO_2 and was replaced with a new one when O_2
187 exceeded 5% of the volume due to gas volume depletion. The nPCE controls were operated in the same
188 conditions as the polarized systems but without monitoring the current density. The only available energy
189 source in the nPCE controls was the organic C fed at the beginning of the enrichment.

190 In the second enrichment method, diazotrophic autotrophic bacteria were enriched in inorganic
191 medium supplemented with H_2 as sole energy source. These enrichments on H_2 were obtained by pre-
192 enriching in strict autotrophic bacteria using 50 ml of inorganic medium in a 120 ml bottle. The
193 headspace consisted of a mixture of 75/15/8/2 (v:v:v:v) $H_2/CO_2/N_2/O_2$ at an initial pressure of 1.5 bar
194 (absolute). Two two-weeks batches (30 days) were performed with NH_4Cl (1g/L) as nitrogen source in the
195 first stage of this enrichment. This nitrogen source was then replaced by N_2 as only N source to enrich N_2 -
196 fixing bacteria in the second stage of enrichment. Centrifugation (10min, 7500 RPM, ~7500g) of 80% of

197 the initial medium (40mL) was done at each subculture every 15-20 days. The pellets obtained after
198 centrifugation were suspended in 5mL of sterile medium before being used for subculturing.

199 **Medium analyses**

200 NH_4^+ , NO_2^- and NO_3^- concentrations were measured using a Gallery+ sequential analyzer (Thermo
201 Fisher Scientific). Two mL of samples were centrifuged at 13500 RPM (~12300g) and then filtered to
202 0.2 μm with nylon membranes before being stored at 4°C. The remaining pellets were stored at -20°C and
203 used for community analysis. VFAs and other carbon compounds were measured on Clarus 580 GC
204 equipped with FID and a Dionex UltiMate 3000 HPLC as described elsewhere (Carmona-Martínez et al.,
205 2015; Moscoviz et al., 2019).

206 Total nitrogen was measured using a CHNS Flashsmart elemental analyzer (Thermo Fisher Scientific).
207 The sample (approximately 2.5 mg) was weighed and was introduced into the oxidation/reduction
208 chamber of the analyzer. 200 mL of medium were sampled at each medium change. These samples were
209 dried for 4-5 days at 60°C. The samples were then freeze-dried and then grounded with a mortar. Two to
210 four mg of each sample was used in the CHNS analyzer. The nitrogen content was then compared to the
211 dry weight measured before freeze-drying to determine the mass of nitrogen in the medium. No CHNS
212 analysis was performed on H_2 -based enrichment due to a low culture volume (50mL). A C/N ratio was
213 then calculated to evaluate the state of the biomass and possible inhibitions of N_2 fixation (Khan et al.,
214 2016; W. Zhang et al., 2020).

215 Nitrogen present in the biomass (biofilm and planktonic) was estimated by calculation from 16S rDNA
216 qPCR. The rrnDB-5.7 database was used to estimate the actual bacterial amount from 16S rDNA qPCR
217 using theoretical 16S rDNA copies per strain, genus or family (Stoddard et al., 2015). Then, the theoretical
218 number of bacteria was used to determine the nitrogen content in the biomass using the theoretical
219 average dry mass of an *Escherichia coli* cell of 216×10^{-15} g/bacterium and with a theoretical relative mass
220 of nitrogen in microbial biomass, ie. 11.4% according to the average biomass formula $\text{CH}_{1.8}\text{O}_{0.5}\text{N}_{0.2}$ (Heldal
221 et al., 1985; Loferer-Krößbacher et al., 1998). The nitrogen present in the biomass was therefore
222 estimated using the formula below:

223
224 Eq. 6
$$N_{(in\ biomass)} = theoretical\ bacteria\ count \times mass\ E.\ coli \times relative\ mass\ of\ N\ in\ biomass$$

225
226 With $N_{in\ biomass}$ the nitrogen concentration in the medium from biomass in mg_N/L , the *theoretical*
227 *bacteria count* based on the bacteria concentration in each enrichment (number of bacteria/L), *mass E.*
228 *coli* a constant of 2.16×10^{-10} $\text{mg}/\text{cell}_{E.\ coli}$ and *relative mass of N in bacteria* is 11.4% of the dry mass.

229 **Gas analysis and acetylene reduction assay (ARA)**

230 CO_2 , H_2 and N_2 used in the headspace of the enrichments were provided at laboratory grade. Pure
231 ethylene was also supplied for calibration of the gas chromatography ethylene measurement.

232 Headspace compositions and pressures were analyzed every 1-2 days. The pressure was manually
233 measured with a Keller LEO 2 manometer (KELLER AG, Wintherthur, Switzerland). Gas analyses were
234 carried out on a Perkin Elmer Clarus 580 GC equipped with RT-Q-Bond and RT-MSieve 5Å columns with a
235 TCD allowing the quantification of H_2 , CO_2 , N_2 , O_2 and CH_4 with Ar as carrier gas as described by A.
236 Carmona-Martínez (Carmona-Martínez et al., 2015). Acetylene and ethylene were measured using a
237 Perkin Elmer Clarus 480 GC equipped with RT-U-Bond and RT-MSieve 5Å columns with TCD and He as
238 carrier gas as described in a previous work (Carmona-Martínez et al., 2015).

239 The acetylene reduction assay (ARA) was performed during enrichment to quantify the rate of N_2
240 fixation using the ability of nitrogenases to reduce acetylene to ethylene. This reaction occurs at a rate
241 proportional to the rate of N_2 fixation according to the theoretical ratio $\text{C}_2\text{H}_2:\text{N}_2$ (3:1) (Bergersen, 1970).
242 The ARA was performed only after 18 batch cycles for H_2 enrichment and 11 batch cycles in polarized
243 cathode enrichment fed with CO_2 (340 days). A specific N_2 -fixing activity was then calculated with the N_2 -
244 fixing bacteria measured by quantification of the *nifH* gene used as a marker for these bacteria. The
245 acetylene used for the acetylene reduction assay (ARA) was obtained by adding calcium carbide (CaC_2) in
246 water and recovered in a bag. The acetylene concentration in the bag was then measured by gas
247 chromatography. Gas from the bag was added to each enrichment to reach a composition of 10% V/V
248 acetylene and an equivalent amount of gas was removed from the headspaces. Ethylene production was

249 then daily monitored for 7 days in the microbial electrolysis systems (PCE and nPCE) and 15 in the H₂
250 bottles by the Perkin Elmer Clarus 480 GC with TCD. To ensure separation of ethylene from CO₂ on the
251 RT-U-Bond column, a CO₂ trap with sodium hydroxide (6M NaOH) was used at the time of sampling. After
252 the ARA method was completed, the headspaces were flushed with N₂ and the gas recycling system was
253 changed.

254 **Community sequencing and biomass quantification**

255 The microbial communities were quantified using the 16S rDNA qPCR to determine the total bacterial
256 concentration and *nifH* gene qPCR for N₂-fixing bacteria. In parallel, 16S rDNA sequencing was performed
257 to identify major members of each community. This sequencing was also necessary to convert the
258 amount of 16S rDNA to total bacteria using the rrnDB-5.7 database. To analyze the communities present
259 in suspension, 1.8 mL of sample were collected for qPCR. For the cathodes, 1 cm² was recovered at
260 several times. The piece of carbon felt was then chopped with a sterile scalpel before being immersed in
261 20 mL of sterile inorganic media. 1.8 mL was then recovered after shaking 20 mL of medium to resuspend
262 as much biomass as possible. These samples were then centrifuged 10 min 13500 RPM (12340g). The
263 supernatant was discarded and the pellets retained for DNA extractions. After qPCR, the concentrations
264 measured in the electrode samples were expressed considering the volume of medium.

265 Genomic DNA was extracted using the PowerSoil™ DNA Isolation Sampling Kit (MoBio Laboratories,
266 Inc., Carlsbad, CA, USA) according to the manufacturer's instructions. The qPCR amplification program
267 was performed in a BioRad CFX96 Real-Time Systems C1000 Touch thermal cycler (Bio-Rad Laboratories,
268 USA). For the analysis of total bacteria, primers 330F (ACGGTCCAGACTCCTACGGG) and 500R
269 (TTACCGCGCTGCTGGCAC) were used. For the bacteria qPCR mix: SsoAdvanced™ Universal SYBR Green
270 Supermix (Bio-rad Laboratories, USA), primer 330F (214 nM), primer 500R (214 nM), 2 µL of DNA, and
271 water were used to a volume of 12 µL. The qPCR cycle was as follows: incubation for 2 min at 95°C and 40
272 cycles of dissociation (95°C, 10 s) and elongation (61°C, 20 s) steps. The results were then compared to a
273 standard curve to obtain the copy number of the target in the sample. Both the 16S rDNA concentration
274 of the PCE media and the cathodes are considered in the calculation of the total 16S rDNA concentration
275 of the PCE. These concentrations are used as an indicator of the biomass present and the use of a
276 database of the number of 16S operons per bacterial genome was used to estimate the actual amount of
277 bacteria.

278 The presence of N₂-fixing bacteria was monitored by qPCR of the *nifH* gene of the Fe-Fe subunit of
279 nitrogenases (Dos Santos et al., 2012; Gaby & Buckley, 2012). All qPCR amplification programs were
280 performed in a BioRad CFX96 Real-Time Systems C1000 Touch thermal cycler (Bio-Rad Laboratories,
281 USA). The primers PolF-TGCGAYCCSAARGCBGACTC and PolRmodify reverse-AGSGCCATCATYTCRCCGGA
282 were used (Poly et al., 2001). The mixture: 6µl SsoAdvanced™ Universal SYBR Green Supermix (Bio-rad
283 Laboratories, USA), F primer (500 nM), R primer (500 nM), 2 µL of DNA and water was used up to a
284 volume of 12 µL. The qPCR cycle was as follows: incubation for 2 min at 95°C and 40 cycles of dissociation
285 (95°C, 30 s) and elongation (60°C, 30 s) steps. Then, the results were compared to a standard curve to
286 obtain the number of copies of the target in the sample. These two quantifications allow us to calculate
287 the ratios of N₂-fixing bacteria per total bacteria of the enrichments at different points to track the
288 enrichment of N₂-fixing bacteria. This ratio can also help us to derive hypotheses on the functioning of
289 our communities that can be completed by the analysis of the communities during sequencing.

290 After quantification, our enriched communities were sequenced according to their 16S rDNA and the
291 results are available on NCBI repository PRJNA838547, Biosample SAMN28447998-SAMN28448066. The
292 V3-V4 region of the 16S rDNA was amplified using universal primers as reported elsewhere (Carmona-
293 Martínez et al., 2015). The PCR mixture consisted of MTP Taq DNA Polymerase (Sigma-Aldrich, Germany)
294 (0.05 u/µL) with enzyme buffer, forward and reverse primers (0.5 mM), dNTPs (0.2 mM), sample DNA (5-
295 10 ng/µL), and water to a final volume of 60 µL. 30 cycles of denaturation (95°C, 1 min), annealing (65°C,
296 1 min), and elongation (72°C, 1 min) were performed in a Mastercycler thermal cycler (Eppendorf,
297 Germany). A final extension step was added for 10 min at 72 °C at the end of the 30th amplification cycle.
298 PCR amplifications were verified by the 2100 Bioanalyzer (Agilent, USA). The GenoToul platform
299 (Toulouse, France <http://www.genotoul.fr>) used an Illumina Miseq sequencer (2 x 340 bp pair-end run)
300 for the sequencing reaction. The raw sequences obtained were analyzed using bioinformatic tools.

301 Mothur version 1.39.5 was used for cleaning, assembly and quality control of the reads. Alignment was
302 performed with SILVA version 128 (the latter was also used as a taxonomic contour).

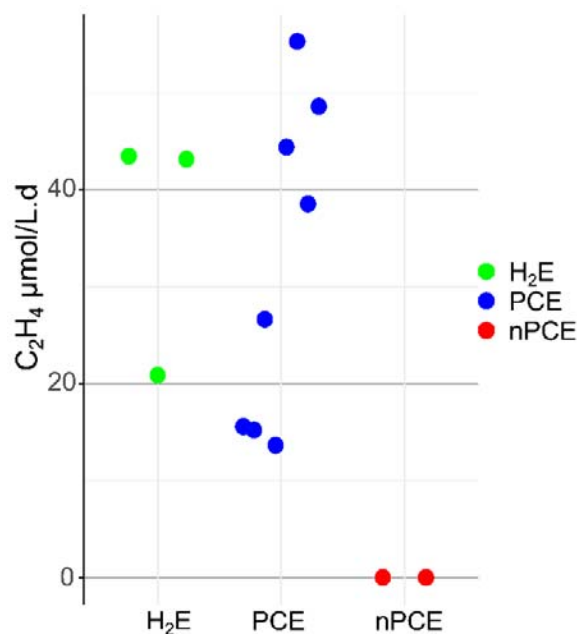
303 Data analysis

304 All results were analyzed using R (4.2.0) and Rstudio (2022.07.1) for calculations and graphics. The
305 Tidyverse package was used for data manipulation (*Tidyverse*, n.d.). The packages ggplot2, ggpubr, scales,
306 cowplot, corrplot and palettetown were used for the graphical representations. Visual representation of
307 bacterial relative abundances was performed with the phyloseq package (McMurdie, 2011/2023).
308 Inkscape software was also used to edit the graphs when necessary. The uncertainties shown for the
309 values presented are standard deviations. All data and scripts used here are available online (Rous, 2023).
310

311 Results and discussion

312 Nitrogen fixation after 340 days of enrichment

313 N₂ fixation was quantified at the day 340 of the enrichment using acetylene reduction assays (ARA).
314 This assay was performed in H₂-fed bottle enrichments (named 'H₂E'), in polarized cathode enrichment
315 (named 'PCE') and in the non-polarized cathode enrichments as controls (named 'nPCE'). As shown in
316 Figure 1, the ARA results confirmed the N₂ fixation capacity of the enriched communities (Bergersen,
317 1970). This indicates that the cathode and/or H₂ was used as energy sources for N₂ fixation both in PCE
318 and in H₂E bottles. The average rates were similar in both enrichment methods with 32±17 μmolC₂H₄/L.d
319 in PCE and 36±13 μmolC₂H₄/L.d in H₂E bottles. The PCE corresponding N₂ fixation rates ranged from 0.12
320 mg_{Nfixed}/L.d (minimum) to 0.51 mg_{Nfixed}/L.d (maximum), which is consistent with the rate of 0.2
321 mg_{Nfixed}/L.d estimated by Rago et al. (Rago et al., 2019) and also with N₂ fixation rates reported for soil
322 bacteria (Hardy et al., 1973; Kifle & Laing, 2016). Despite these significant N₂ fixation rates and the long
323 duration of the experiments, the rate of ammonium production in solution remained lower than 0.07
324 mg_N/L.d at the day 340 (Table 1), indicating that most of the fixed N₂ was probably rapidly used by
325 bacteria.
326



327

328 **Figure 1** - Reduction rate of acetylene in μmol C₂H₄/L.d in the different reactors after 340 days of operation . or H₂
329 condition, 3 bottles were used for the acetylene reduction assay with one injection for each bottle, i.e. 3 measurements.
330 For PCE, 2 reactors were used and 4 injections were made to validate the repeatability of the measurement when C₂H₄

331 which gives 8 measurements for each of these two conditions. For nPCE, 2 reactors were used which gives 2
332 measurements for each conditions.

333 The ability of the microbial communities to fix N_2 was also assessed by qPCR of the *nifH* gene (Dos
334 Santos et al., 2012; Pogoreutz et al., 2017). The amounts of N_2 -fixing bacteria after 340 days of
335 enrichment are reported in Table 1. The average *nifH* gene concentration in PCE was estimated at $7.8 \cdot 10^7$
336 copies_{*nifH*}/mL, two orders of magnitude higher than the average concentration of $8.3 \cdot 10^5$ copies_{*nifH*}/mL
337 measured in the H_2 enrichment bottles. This observation was surprising since N_2 -fixation rates were
338 similar in both configurations (Figure 1). This suggests that the fixation rate per *nifH* copy was much
339 higher in H_2E than in PCE. The estimated specific activities per *nifH* copy were indeed of 0.2 ± 0.3
340 $\mu\text{mol}_{C_2H_4}/10^8$ copies_{*nifH*}.d in the PCE and 2.1 ± 0.7 $\mu\text{mol}_{C_2H_4}/10^8$ copies_{*nifH*}.d in H_2 enrichment bottles (Table
341 1). Furthermore, the comparison between *nifH* gene and 16S rRNA gene copy numbers gives an idea of
342 the proportions of nitrogen fixing bacteria in each microbial community. Interestingly, this proportion
343 was 18% in H_2 enrichment bottles that was four times higher than the value of 4.6% in PCE (Table 1).
344 Therefore, N_2 -fixing bacteria constituted a smaller proportion of the bacterial populations in PCE than in
345 H_2E and only a small proportion of the bacteria participated to N_2 fixation in the PCE. In nPCE controls,
346 the biomass was higher than in H_2 enrichment and the *nifH*/16S ratio lower (Table 1). The lack of N_2
347 fixation observed in nPCE indicated that the microbial biomass maintained along the experiment without
348 the need of fixing N_2 . It is assumed that the microbial biomass was partly degraded and used as a source
349 of C and N by other bacteria. Thus, the presence of NH_4^+ in the nPCE was very likely related to cell lysis
350 since no measurable fixation was detected by ARA.

351 **Table 1** - Measurements of average ammonium, *nifH* gene, 16S gene, and *nifH*/16S ratio concentrations averaged at 340
352 days for the three experimental configurations. Averages measured on one batch for the two polarized cathode
353 enrichment (PCE), the two non-polarized Cathode Enrichments (nPCE) and the six H_2 enrichment bottles (H_2E)

	PCE	nPCE	H_2E
$N-NH_4^+$ mg/L.d	0.07 ± 0.01	0.07 ± 0.01	0.04 ± 0.03
<i>nifH</i> gene copies copies/mL	$7.8 \pm 9.5 \cdot 10^7$	$2.5 \pm 2.8 \cdot 10^6$	$8.3 \pm 2.2 \cdot 10^5$
16S rDNA gene copies copies/mL	$1.7 \pm 1.9 \cdot 10^9$	$1.4 \pm 0.2 \cdot 10^8$	$4.6 \pm 1.5 \cdot 10^6$
<i>nifH</i> /16S	3.8 %	1.7 %	19.0 %

354

355 **Current density and Autotrophic/electrotrophic enrichment in polarized cathode enrichment**

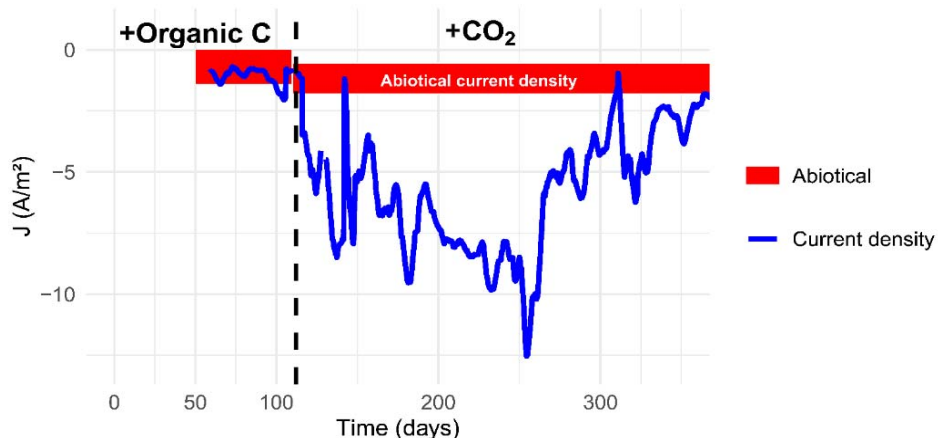
356 The average current density for the two PCE over experimental time is shown in Figure 2. As the
357 current measured at the cathode was negative by convention, a more negative corresponded to a higher
358 reduction activity. Regarding the current densities in the abiotic systems, the average current densities
359 were measured at -0.75 A/m² for two times four days with an organic C source and -1.1 A/m² for 16 days
360 with only CO_2 as the carbon source.

361 The average current density measured in the PCE was not different from the current density
362 measured in the abiotic control (approximately -1 A/m²) for the first 45 days of operation (days 55 to 100
363 of the enrichment). The medium was then changed for a medium with no organic C. An sharp increase in
364 current density to -5 A/m² was observed in the PCE with regards to the average current in the abiotic
365 controls and standard deviation up to -2 A/m² (Figure 2). The higher current density was assumed to be
366 associated to the electroactive activity of electron uptake by enriched bacteria. The current density in the
367 PCE then continuously increased until day 250 of the enrichment to reach a value of -15 A/m².

368 The high current consumption observed after 250 days of enrichment strongly suggests a specific
369 enrichment in electroactive bacteria. Indeed, current consumption was 5 to 10 times higher than in
370 average for the abiotic controls, and was likely due to the direct use of electrons by bacteria in a cathodic
371 biofilm as proposed by Z. Zaybak et al (Zaybak et al., 2013). Compared to the current densities obtained
372 Rago et al. (Rago et al., 2019) in the order of magnitude of -10 mA/m² at the same potential (-0.7 vs SHE),

373 the current densities observed here (-5 to -10 A/m²) were about 1000 times higher. These current density
374 levels are close to those measured by Zhang et al. (L. Zhang et al., 2022) who reported a maximum of -10
375 A/m² at the same applied potential.

376 After 230 days, power failures occurred, interrupting temporarily the current supply to the cathodes.
377 An important decrease of the current density was observed afterwards, down to -5 A/m² after 260 days
378 and -3 A/m² after 320 days. The lower current density reflected a change in the functioning of the
379 microbial communities, leading to less electron exchange with the cathode.
380



381

382 **Figure 2** - Mean current density measured for the two PCE (blue line). Levels shown in red correspond to theoretical
383 mean current density and standard deviation estimated from two abiotic electrochemical systems current densities. For
384 abiotic electrochemical system, one batch of 2 days were made with Organic C and one batch of 16 days with CO₂. The
385 peaks observed are due to the batch operation of the PCE with disturbances each time the medium was renewed. Power
386 failures occurred at 230 days and 260 days. The time indicated on the x axis corresponds to the experimental time starting
387 at day 0 of the enrichment where soil samples were first introduced in the bottles with a medium containing organic C. Day
388 55 corresponds to the start of microbial electrochemical system with the precultured communities. The dashed line on day
389 110 corresponds to the passage on CO₂ as the sole carbon source in PCE.

390 **Biomass quantification**

391 Bacterial biomass was monitored in the enrichments by measuring 16S rDNA concentrations by qPCR
392 (Figure 3). At day 131 (18 days after switching from organic C to CO₂), the average 16S rDNA
393 concentrations measured in the polarized cathode enrichment (PCE) and in the non-polarized cathode
394 enrichment (nPCE) controls were $4.6 \pm 0.4 \cdot 10^9$ and $4.2 \pm 1.2 \cdot 10^9$ copies/16S rDNA/mL, respectively. These
395 concentrations corresponded to $9.4 \pm 1.0 \cdot 10^8$ and $8.0 \pm 1.5 \cdot 10^8$ bacteria/mL, respectively, as presented in
396 Figure 3. These bacteria concentrations resulted from the first enrichment phase with organic C. During
397 this phase, organic substrates were used as carbon and energy sources for biomass growth in both
398 configurations (PCE and nPCE). At day 214, the 16S rDNA concentration in the PCE was estimated at
399 $3.3 \pm 2.1 \cdot 10^9$ bacteria/mL, corresponding to a biomass increase by a factor of 3.5 between 131 and 214
400 days (Figure 3). At the same time, the bacterial concentration dropped in nPCE from $8.0 \pm 1.5 \cdot 10^8$
401 bacteria/mL to $3.0 \pm 0.8 \cdot 10^8$ bacteria/mL. This drop was explained by the lack of available energy source
402 for growth, which led to a sharp decrease of the bacterial populations. At day 214, the 16S rDNA
403 concentration in PCE was therefore 11-fold higher than in nPCE controls. This difference is consistent
404 with the difference reported by Rago *et al.* (Rago *et al.*, 2019) between polarized and non-polarized
405 conditions, with electroactive biocathodes enriched in autotrophic diazotrophic bacteria. These results
406 suggested that the enriched microbial communities were able to use the electrodes polarized at -0.7 V vs.
407 SHE as sole energy sources to grow while fixing N₂.

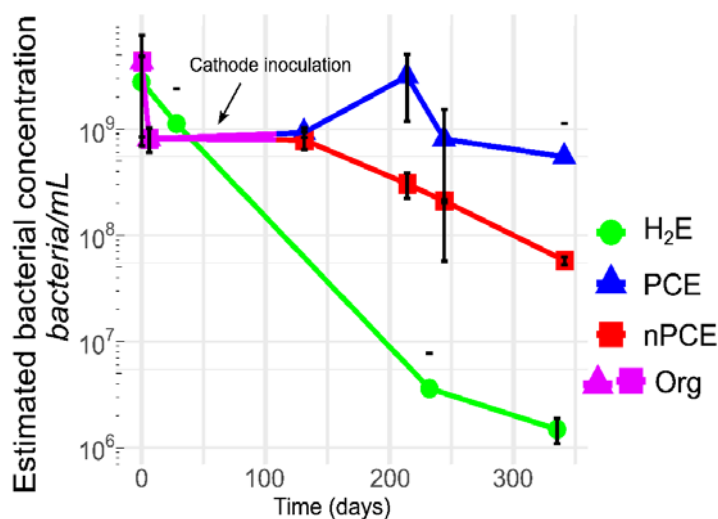
408 In the H₂-fed enrichment (H₂E) bottles, the 16S rDNA concentration steadily decreased along the
409 experiment. The concentration decreased from $1.1 \pm 1.3 \cdot 10^9$ bacteria/ml at the beginning of the
410 enrichment down to $1.3 \pm 0.3 \cdot 10^6$ bacteria/ml after 340 days (Figure 3). These concentrations appear
411 lower than the biomass concentrations observed in the PCE medium at the same time of enrichment, ie.
412 $4.5 \pm 5.9 \cdot 10^6$ bacteria/mL at day 244 and $8.6 \pm 8.8 \cdot 10^6$ bacteria/mL at day 340. These results confirm that

413 bacterial growth was higher on the cathodes than in an H₂ supplied environment. It was therefore
414 concluded that the PCE provided more favorable environment for biomass growth than H₂ fed bottles as
415 the surface provided by the electrode was likely favorable for biofilm growth.

416 We also calculated the *nifH*/16S ratio representing the part of bacteria able to fix N₂ among the total
417 bacteria. A ratio of 0.06% of *nifH* gene copies per 16S rDNA copy was measured for samples at the very
418 beginning of enrichment, both for H₂E and PCE. After 131 days, corresponding to the switch to CO₂ as
419 sole C-source, this level increased to 3.1% in PCE and 1.5% in nPCE control. These results are consistent
420 with an enrichment in diazotrophic bacteria during the enrichment phase on organic carbon (Bowers et
421 al., 2008). The bacterial enrichment in nPCE was likely possible as the organic C was used by the bacteria
422 as energy source. After 214 days, the level decreased to 1.9% in PCE but remained higher than the level
423 at the beginning of enrichment. This variation suggests interactions within the community that favored
424 the growth of non-N₂ fixing bacteria after the shift to CO₂ as sole C-source. After 340 days, the ratio of
425 *nifH* to 16S rDNA was 3.8% as presented in Table 1. In parallel, a ratio of *nifH* to 16S rDNA of 90% was
426 measured for H₂E at 244 days. Therefore, most of the bacteria were able to fix N₂ in H₂E bottles,
427 confirming the efficient enrichment in diazotrophic bacteria (Bowers et al., 2008). Given the loss of
428 biomass observed in H₂E during the experiment (Figure 3), this high ratio corresponded likely to the
429 surviving bacteria that were selected on their ability to fix N₂. The ratio measured in these H₂E then
430 decreased down to 19%, suggesting a decrease in N₂-fixing bacteria biomass.

431 As previously mentioned, after 230 days, power failures occurred and interrupted the polarization of
432 the electrodes. These interruptions impacted the microbial communities with a decrease in biomass
433 concentration to $8.1 \pm 7.6 \cdot 10^8$ bacteria/mL at 244 days and $5.5 \pm 6.0 \cdot 10^8$ bacteria/mL after 340 days
434 compared to the concentration of $3.3 \cdot 10^9$ bacteria/mL measured at 214 days. At the same time, the
435 *nifH*/16S rDNA ratio increased up to 5%, indicating that N₂-fixing bacteria were more resistant.
436 Nevertheless, a decrease was observed in *nifH* quantities, from $2.3 \cdot 10^8$ copies_{*nifH*}/mL after 214 days to 7.8
437 10^7 copies_{*nifH*}/mL after 340 days.

438



439

440 **Figure 3** - Bacteria concentrations over time in the different enrichments calculated from 16S rDNA qPCR
441 quantifications in bulk and biofilm. Green disks correspond to H₂ enrichments in bottles, blue triangles correspond to
442 polarized cathode enrichment (PCE), red squares correspond to controls in non-polarized cathode enrichment (nPCE). The
443 partially purple symbols marked Org correspond to the first phases of enrichment with organic C for the PCE and nPCE. The
444 arrow indicates the transition from bottle enrichments to cathode enrichments in microbial electrochemical systems for
445 PCE and nPCE. Error bars correspond to the calculated standard deviation.

446 **N quantification and coulombic efficiency**

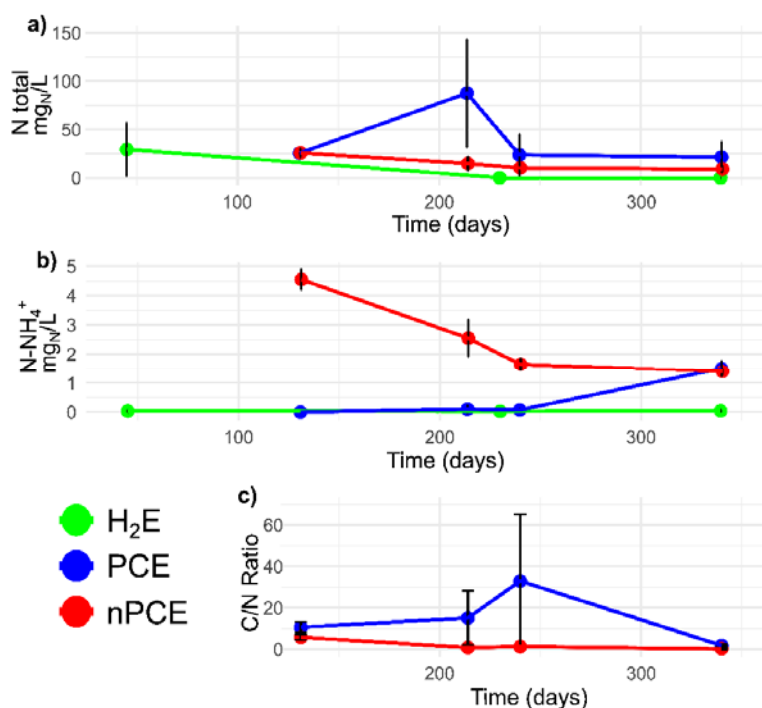
447 Total N contents of the different experiments are shown in Figure 4a. The total N corresponded to the
448 sum of the nitrogen measured in the liquid phase by N-ion concentration analysis (N-NH₄⁺, N-NO₃⁻, N-
449 NO₂⁻), in the medium by CHNS elemental analysis for PCE and nPCE, in the suspended biomass from qPCR
450 results only for H₂E where the dry mass was not measured, and on the electrode based on the bacterial

451 concentrations. The total N concentration was estimated after 131 days of enrichment (ie. before the
452 shift to CO₂ as sole C source) at 25.5±0.4 mg_N/L and 25.8±4.7 mg_N/L in the PCE and in the nPCE controls,
453 respectively. After 214 days of enrichment, total N increased up to 87.6±56.1 mg_N/L in the PCE with
454 regards to the low value of 14.8±7.0 mg_N/L in the nPCE controls. Ammonium represented only a small
455 fraction of the total N in the PCE. The maximum ammonium concentration observed at a batch end in the
456 PCE was 1.5±0.3 mg_N/L at the day 340 of the enrichment in comparison with the maximum value of
457 4.5±0.4 mg_N/L found in nPCE control after 131 days (1.4 mg_N/L at the day 340) .(Figure 4b). The average N
458 fraction in the form of ammonium was therefore of 12% in nPCE and only 1.6% in PCE. It was thus
459 assumed that the higher level of ammonium in nPCE was related to the decay of biomass in absence of
460 energy sources. In counterpart, the ammonium produced by N₂ fixation in the PCE was likely directly used
461 for protein synthesis as suggested elsewhere (Temple et al., 1998). In addition, nPCE N-NO₃⁻
462 concentrations were 5 to 15 times lower than N-NH₄⁺ concentrations with maximum values of 0.9 mg_N/L
463 N-NO₃⁻ in the nPCE control and 0.2 mg_N/L N-NO₃⁻ in PCE. An average concentration of 0.1±0.2 mg_N/L N-
464 NO₃⁻ in H₂E bottles was also observed. NO₂⁻ concentrations were negligible.

465 The C/N ratios are shown in Figure 4. C/N ratios in the PCE were around 10 after 131 and 214 days in
466 comparison with ratio of 5 to less than 1 in the nPCE control. These ratios are consistent with the
467 theoretical ratio of 8 to 10 assumed for microbial biomass (Goldman et al., 1987; Heuck et al., 2015;
468 Yaghoubi Khanghahi et al., 2021). In contrast, the low ratios in nPCE indicated that the dry mass was most
469 probably not only composed of microbial cells. Interestingly, the level of C/N reached 30/1 in the PCE
470 after 244 days of enrichment. Such increase could be related to the release of carbon molecules such as
471 exopolysaccharides. the C/N ratio finally dropped down to 1.8 after 340 days, confirming cell lysis as
472 previously suggested.

473 The H₂ enrichment bottles (H₂E) showed an average N-NH₄⁺ accumulation of 35.6±36 µg_N/L after 131
474 days and an average of 0.1±0.2 mg_N/L over the duration of enrichment. This concentration represented a
475 small fraction of the total N at the very beginning of the enrichment, with an estimated concentration of
476 29.4±28 mg_N/L. The N concentration decreased during the enrichment, which is consistent with the
477 biomass loss as shown in Figure 3. H₂E were therefore less efficient for N₂ accumulation than polarized
478 cathode enrichment, with a lower microbial biomass production.

479



480

481 **Figure 4** - (a) Total N concentration based on N measured in dry weight from medium samples for polarized cathode
482 enrichment (PCE) and non-polarized cathode enrichment (nPCE) and estimated from biomass for H₂-fed enrichment (H₂E),

483 on ions ($N-NH_4^+$, $N-NO_3$, $N-NO_2$) concentrations, and on N estimated from the biomass in biofilm for PCE and nPCE, (b) $N-NH_4^+$
 484 concentration in H₂E, PCE and nPCE, (c) C/N ratio measured from dry weight of medium of PCE and nPCE. The error
 485 bars presented are the standard deviations calculated from the different replicates (2 PCE, 2 nPCE, 3-6 H₂E bottles).

486 Current densities and rates of acetate production, N₂ fixation and biomass growth are shown in Table
 487 2. Coulombic efficiencies associated with each reaction were estimated based on these results (Table 2).
 488 During the first 214 days of enrichment, 0.6 to 3.3% of the electrons were used for N₂ fixation in the two
 489 PCE. In comparison, efficiencies of 0.5% and 20% for NH_4^+ synthesis was reported in two recent works
 490 carried out under similar conditions (Yadav et al., 2022; L. Zhang et al., 2022). As the amount of fixed N
 491 was highly dependent on biomass accumulation, negative results were obtained at day 244 when
 492 biomass started to decrease. The electrons used at the cathode for biomass synthesis during the first
 493 period (131 to 214 days) accounted for 2.8% and 17.3% in the two PCE. These high coulombic efficiencies
 494 were probably also associated to microaerophilic conditions. As acetogenic bacteria do not tolerate the
 495 presence of oxygen, dissolved O₂ was very probably consumed in some part of the biofilm, leaving other
 496 parts in strict anaerobic conditions more favorable for acetogenic bacteria growth.

497 The H₂ recovered in the headspace of the PCE accounted for 12 to 22% of the electrons supplied to
 498 the cathode as presented in Table 2. Therefore, H₂ was not related to the biological activity and mostly
 499 resulted from an abiotic reaction at the cathode.

500 Interestingly, a significant production of acetate was also observed. An average rate of 149.1
 501 $\mu\text{mol/L.d}$ and 421.6 $\mu\text{mol/L.d}$ were measured in both PCE for the period from day 131 to day 214, as
 502 presented in Table 2. Acetate production almost stopped with the power failures with acetate measured
 503 only on one to two batches per PCE. This decrease correspond to rate of 61.0 $\mu\text{mol/L.d}$ and 57.4 $\mu\text{mol/L.d}$
 504 of acetate in both PCE. Acetate production accounted for 7.9 and 39% of the cathodic electrons during
 505 the first period (up to 214 days) and for less than 5% after power failures. To explain the decrease in
 506 acetate production, biomass growth and power consumption, it was hypothesized that acetate
 507 production might have been due to a specific loss of members able to fix CO₂, and more especially
 508 electrorophic bacteria, within the enriched community. Thus, with acetate no longer being produced,
 509 heterotrophic bacteria did not have enough organic C to sustain their growth, causing their decrease.
 510 Therefore, electrorophic bacteria responsible for CO₂ fixation and heterotrophic bacteria that could also
 511 be H₂ dependent for N₂ fixation were greatly affected, leading to a decrease in the reduction reactions at
 512 the cathode and in current density. In addition, acetate was not found in the H₂E bottles, indicating the
 513 absence of acetogenesis and an important difference in microbial pathways and/or communities.

514 **Table 2** - Current densities, rates and coulombic efficiencies for the two polarized cathode enrichment (PCE) over two
 515 different periods of current consumption with CO₂ as sole carbon source. During the first period (131-214 days) current
 516 consumption increased, whereas during the second period (>215) current consumption decreased after several power
 517 outages (see Figure 2).

		131-214 days		> 215 days	
		PCE 1	PCE 2	PCE 1	PCE 2
J A/m ²	Mean	7.7±3.1	5.9±2.4	6.2±4.1	3.8±2.2
	Max	28.2	11.3	19.5	9.9
Acetate $\mu\text{mol/L.d}$	Mean	149.1±203.1	421.6±216.7	57.4±151.8	61.0±106.5
N $\mu\text{mol/L.d}$	N- NH_4^+	0.108±0.225	0.155±0.249	2.0±1.4	1.5±1.9
	N Bulk Dry weighth	10.3±6.0	27.5±13.4	9.0±6.4	12.1±6.4
	N Biomass theoretical (16S/bact)	16.7	80.4	-3.0	-7
Biomass bact/L.j	Bulk	0.4 ± 0.5 10 ⁹	3.5 ± 2.0 10 ⁹	0.4±0.5 10 ⁹	0.2±0.1 10 ⁹

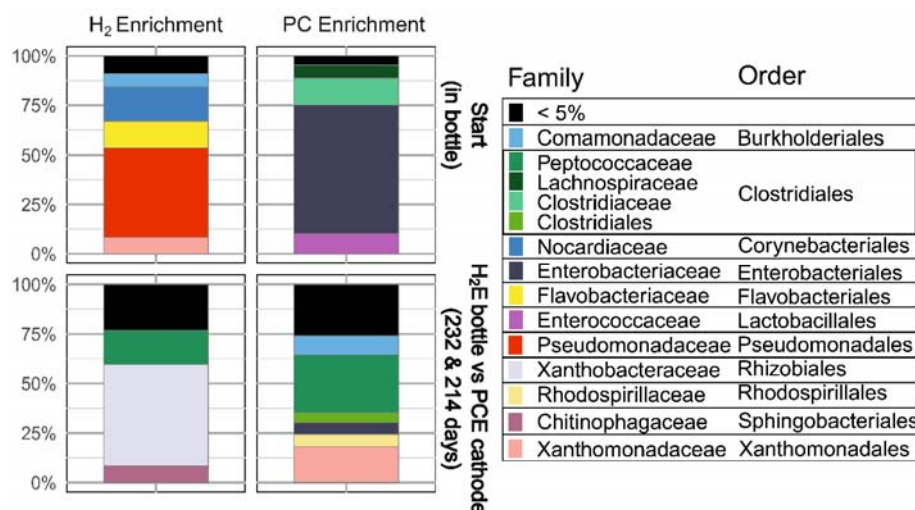
	Cathode	$0.9 \cdot 10^{10}$	$4.6 \cdot 10^{10}$	$-2.6 \pm 3.5 \cdot 10^{10}$	$-5.9 \pm 7.8 \cdot 10^{10}$
Coulombic efficiency %	CO ₂ to Acetate	7.9±9.5	30.9±8.9	2.1±5.6	5.0±6.6
	H ⁺ to H ₂	22.3±15.4	12.1±8.8	9.4±13.5	14.4±14.4
	N ₂ fixation	0.6±0.2	3.3±0.8	0.2±1.0	-0.5±2.2
	Biomass growth	2.8±0.5	17.3±5.3	-2.5±4.0	-8.3±14.2
	Total	33.6±14.4	63.6±9.0	9.2±16.5	10.5±18.8

518

519 Microbial communities

520 16S rDNA sequencing was performed at the beginning of the culture, and at 214 or 232 days of
 521 enrichment in polarized cathode enrichment (PCE) and in H₂-fed enrichment bottles, respectively. The
 522 sampling days were selected because they were associated to a high microbial activity (high current
 523 densities and high biomass concentrations). In H₂E, the *nifH*/16S abundance ratio was also maximum
 524 (90%) at day 232. Averages of relative abundances of the bacterial families are shown in Figure 5.

525 At the beginning of the PCE in bottles fed with organic C, communities were strongly dominated by
 526 only four families accounting for more than 96% of total sequences: *Clostridiaceae* (14%),
 527 *Enterobacteriaceae* (65%), *Enterococcaceae* (10%) and *Lachnospiraceae* (7%). A dominance of the
 528 *Enterobacteriaceae* family (mainly of the *Citrobacter* genus) was observed. All these families, and in
 529 particular *Clostridiaceae* and *Enterobacteriaceae* families are supposed to possess numerous genera
 530 capable of N₂ fixation and possessing the *nifH* genes (Huang et al., 2019; Lin et al., 2012; Minamisawa et
 531 al., 2004). This observation indicated a rapid selection of bacteria having the capability of N₂-fixation at
 532 the early stage of enrichment.



533

534 **Figure 5** - Average relative abundance of bacterial families in H₂E and PCE at the beginning of enrichment (top
535 barplots) and after 214 (for PCE) and 232 days (for H₂E) of enrichment (bottom barplots). Only families with an average
536 relative abundance above 5% in the replicates of one condition are shown.

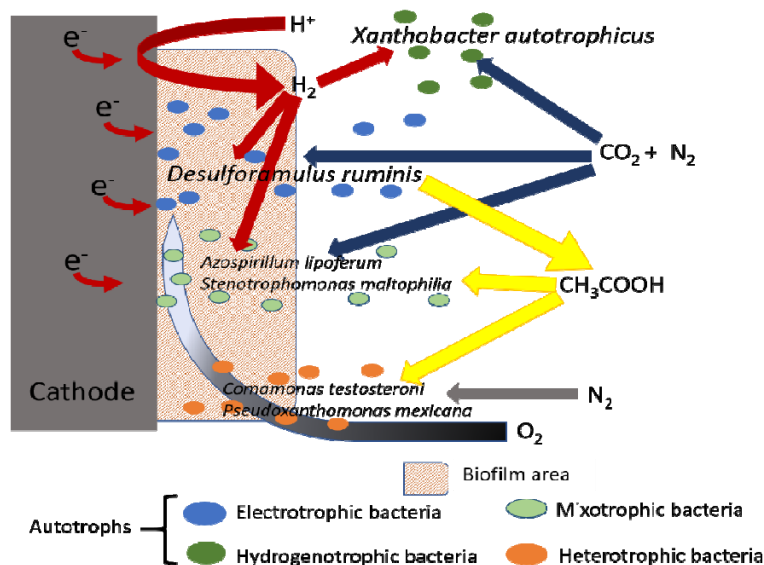
537 In the H₂-based enrichments, and in contrast with the enrichments in PCE, *Pseudomonadaceae* (45%)
538 family was mostly dominant. *Nocardiaceae* (17%), *Flavobacteriales* (14%), *Xanthomonadaceae* (8%) and
539 *Comamonadaceae* (7%) were also present. These families, with the exception of *Flavobacteriales*, are
540 also known to have members possessing the set of genes necessary for N₂ fixation (Dos Santos et al.,
541 2012; Ghodhbane-Gtari et al., 2019; Huda et al., 2022). These families accounted for 77% of the
542 sequences which is high compared to the *nifH*/16S rDNA ratio of less than 1% at the same time point.
543 This suggests that either the *nifH* primers were not adapted to these specific species or that the species
544 found at this point did not possess the genes for nitrogenases. As the H₂E cultures started on a medium
545 containing NH₄Cl, the presence of this source of nitrogen was likely favorable to the growth of non-
546 diazotrophic bacteria.

547 After 214 days of enrichment, PCE major families found in the PCE were affiliated to *Peptococcaceae*
548 (29%), *Xanthomonadaceae* (18%), *Rhodospirillaceae* (6%, *Azospirillum*) and *Comamonadaceae* (10%). A
549 clear shift in microbial communities from the beginning of the experiment was therefore observed. Only
550 *Enterobacteriaceae* (6%) family was maintained although at minor relative abundance. Members of
551 *Clostridiales incertae sedis* absent from original inoculum also appeared on polarized cathode. These
552 families are known to exhibit the role of plant growth promoting bacteria (PGPB). These communities
553 could thus be beneficial when used as living fertilizers (Cassan & García de Salamone, 2008; Rojas-Tapias
554 et al., 2012; Singh et al., n.d.). The *Comamonadaceae* as well as the *Enterobacteriaceae* families mostly
555 include heterotrophic species, which would be consistent with our hypotheses about the existence of
556 interactions between heterotrophic and electrotrophic populations (F. Liu et al., 2011; Wu et al., 2018).
557 More precisely, the *Peptococcaceae* sequences were affiliated to species *Desulforamulus ruminis* (>98%).
558 This species was already described for their ability to fix N₂ (Postgate, 1970). The *Desulforamulus* and
559 *Desulfotomaculum* genera have also several species able to grow with H₂ and CO₂ as energy and C
560 sources (Aullo et al., 2013; Klemps et al., 1985; Zaybak et al., 2013). They were previously reported to be
561 able to produce acetate by CO₂ reduction through the Calvin cycle (Klemps et al., 1985), and some were
562 already found in microbial electrochemical system on a biocathode producing acetate (Zaybak et al.,
563 2013). The other main family, *Xanthomonadaceae*, was represented by several genera with a majority of
564 *Pseudoxanthomonas*. In this genus, some members were identified as N₂ fixers with a need of external
565 organic C source, exhibiting a mixotrophic metabolism depending on the environmental conditions (J. Hu
566 et al., 2022; Ryan et al., 2009). Sequences associated to the *Rhodospirillaceae* family were mainly
567 affiliated to the species *Azospirillum lipoferum* which is able to grow in autotrophy with H₂, CO₂ and N₂
568 (Tilak et al., 1986). This soil bacterium is also known for its role as a PGPB with a capacity to solubilize
569 phosphates, making it a good candidate as a fertilizer (Cassan & García de Salamone, 2008; Tilak et al.,
570 1986). Interestingly, many of the identified bacteria in the polarized cathode enrichment were previously
571 described to possess the N₂-fixing genes and capability. This supports the fact that the primers were not
572 able to amplify the full diversity of *nifH* genes from these communities.

573 E The *Xanthobacteraceae* (51%), *Peptococcaceae* (17%, identified as *Desulforamulus*) and
574 *Chitinophagaceae* (8%) families were found to be dominant in H₂E bottles at day 214. The
575 *Xanthobacteraceae* family was mostly represented by the species *Xanthobacter autotrophicus* which is
576 known as N₂-fixing HOB (Wiegel, 2005). This species was already been used for N₂ fixation by Liu *et al.* (C.
577 Liu et al., 2017) in an hybrid system using the H₂ produced by a cathode. *Xanthobacter autotrophicus* was
578 also found in the medium of the polarized cathode enrichment but in lower abundance (< 5%). Therefore,
579 the community enriched with H₂ was mostly composed of N₂-fixing bacteria, as also supported by the
580 high *nifH*/16S ratio (90%). After 214 days of enrichment, diazotrophic HOB were specifically selected.

581 The presence of mixotrophic and heterotrophic bacteria in the PCE suggested that carbon-based
582 interactions could have occurred. Acetate was the only abundant soluble carbon metabolite found in
583 these enrichments (see Table 2). Therefore, acetate was assumed to be used as intermediate for carbon
584 and electron transfer between electrotrophic or hydrogenotrophic homoacetogens, *e.g.* *Desulforamulus*
585 *ruminis*, and heterotrophic bacteria such as *Comamonas sp.*.

586 Furthermore the low concentration of N-NH_4^+ in the PCE before day 210 (Table 2) was probably due
 587 to its rapid consumption for bacteria growth. Considering these hypothesis, a conceptual scheme of
 588 microbial interactions between the main bacterial families in the PCE was proposed and is presented in
 589 Figure 6. The presence of heterotrophic bacteria and their potential use of O_2 as a final electron acceptor
 590 was also considered. The concentration of dissolved O_2 would have decreased in a deep layer of the
 591 biofilm due to its use by heterotrophic bacteria. A structure of the biofilm in two layers could then be
 592 proposed with a first layer composed mainly of homoacetogens fixed on the cathode and reducing CO_2 to
 593 acetate, and a second layer composed mainly of heterotrophic bacteria using acetate and dissolved O_2 to
 594 sustain their growth. It was assumed that bacteria in the first layer would not access to N_2 that would be
 595 mostly fixed by organisms of the second layer.



597

598 **Figure 6** - Conceptual scheme of microbial interactions occurring in polarized cathode enrichment (PCE) after
 599 enrichment for N_2 fixation with inorganic energy and carbon sources

600

Conclusion

601 Enrichment cultures of N_2 -fixing bacteria were successfully carried out in H_2 -fed bottles (H_2E) and in
 602 polarized cathode enrichment (PCE). Both methods showed significant N_2 fixation after 340 days of
 603 enrichment. The microbial communities selected were able to fix N_2 with CO_2 as sole carbon source and
 604 H_2 or cathodic electrons as sole energy sources. Biomass growth on the cathode up to $4.6 \cdot 10^{10}$
 605 bacteria/L.d is another evidence of autotrophic growth in the PCE while bacterial growth was much lower
 606 in the H_2E . Current consumption confirmed the activity of electrotrophic bacteria in the PCE. As the
 607 coulombic efficiency of N_2 fixation was low with a maximum of 3.3% and considering the low
 608 concentrations of NH_4^+ , it was concluded that the major part of the nitrogen was incorporated into
 609 microbial biomass during the enrichment procedure. Interestingly, acetate was also produced in the PCE
 610 corresponding to a coulombic efficiency of 27%. The related microbial communities found in both
 611 enrichments had some bacterial families in common, but the communities found in the PCE appeared
 612 metabolically more diverse, suggesting probable rich microbial interactions with exchanges of electrons,
 613 carbon and nitrogen between autotrophic, heterotrophic and mixotrophic populations. Several members
 614 of the enriched communities were furthermore reported as plant growth promoting bacteria (PGPB)
 615 which could be interesting for the production of environment friendly fertilizers. To summarize, a
 616 conceptual model of microbial interactions between the main bacterial families found in the
 617 bioelectrochemical system was proposed suggesting a key role of each autotrophic, heterotrophic and
 618 mixotrophic populations in the process of N_2 fixing by cathodic biofilms.
 619

620

Acknowledgements

621 The authors would like to thank the INRAE Bio2E Facility (Bio2E, INRAE,2018. Environmental
622 Biotechnology and Biorefinery Facility, <https://doi.org/10.15454/1.557234103446854E12>) for
623 experimental support.

624

Data and scripts availability

625 Data and scripts are available online on: <https://doi.org/10.57745/ONNGWZ> (Recherche Data gouv)

626

Conflict of interest disclosure

627 The authors declare that they comply with the PCI rule of having no financial conflicts of interest in
628 relation to the content of the article.

629

Funding

630 This work was funded by the French National Research Agency (ANR, ANR-19-CE43-0013 Cathomix).

631

References

- 632 Aullo T, Ranchou-Peyruse A, Ollivier B, Magot, M (2013) *Desulfotomaculum* spp. and related gram-
633 positive sulfate-reducing bacteria in deep subsurface environments. *Front. Microbiol.*, 4, 362.
634 <https://www.frontiersin.org/article/10.3389/fmicb.2013.00362>
- 635 Bagali S (2012) Review: Nitrogen fixing microorganisms. *Int. J. Microbiol. Res.*, 3, 46–52.
636 <https://doi.org/10.5829/idosi.ijmr.2012.3.1.61103>
- 637 Bergersen F J (1970) The quantitative relationship between nitrogen fixation and the acetylene-reduction
638 assay. *Aust. J. Biol. Sci.*, 23(4), 1015-1026. <https://doi.org/10.1071/bi9701015>
- 639 Bowers TH, Reid NM, Lloyd-Jones G (2008) Composition of *nifH* in a wastewater treatment system reliant
640 on N₂ fixation. *Appl. Microbiol. Biotechnol.*, 79(5), 811–818. <https://doi.org/10.1007/s00253-008-1486-2>
- 641 Burgess BK, Lowe DJ (1996) Mechanism of molybdenum nitrogenase. *Chem. Rev.*, 96(7), 2983-3012.
642 <https://doi.org/10.1021/cr950055x>
- 643 Burris RH, Roberts GP (1993) Biological nitrogen fixation. *Annu. Rev. Nutr.*, 13(1), 317-335.
644 <https://doi.org/10.1146/annurev.nu.13.070193.001533>
- 645 Carmona-Martínez AA, Trably E, Milferstedt K, Lacroix R, Etcheverry L, Bernet N (2015) Long-term
646 continuous production of H₂ in a microbial electrolysis cell (MEC) treating saline wastewater. *Water*
647 *Res.*, 81, 149–156. <https://doi.org/10.1016/j.watres.2015.05.041>
- 648 Cassan F, García de Salamone I (2008) *Azospirillum: Cell physiology, plant response, agronomic and*
649 *environmental research in Argentina*. ISBN 978-987-98475-8-9.
- 650 Chakraborty T, Akhtar N (2021) Biofertilizers: Prospects and Challenges for Future. In *Biofertilizers* (pp.
651 575–590). John Wiley & Sons, Ltd. <https://doi.org/10.1002/9781119724995.ch20>
- 652 Cherkasov N, Ibhaddon AO, Fitzpatrick P (2015) A review of the existing and alternative methods for
653 greener nitrogen fixation. *Chem. Eng. Process.*, 90, 24–33. <https://doi.org/10.1016/j.cep.2015.02.004>
- 654 Deng J, Iñiguez JA, Liu C (2018) Electrocatalytic nitrogen reduction at low temperature. *Joule*, 2(5), 846–
655 856. <https://doi.org/10.1016/j.joule.2018.04.014>
- 656 Dos Santos PC, Fang Z, Mason SW, Setubal JC, Dixon R (2012) Distribution of nitrogen fixation and
657 nitrogenase-like sequences amongst microbial genomes. *BMC Genomics*, 13, 162.
658 <https://doi.org/10.1186/1471-2164-13-162>
- 659 Franche C, Lindström K, Elmerich C (2009) Nitrogen-fixing bacteria associated with leguminous and non-
660 leguminous plants. *Plant Soil*, 321, 35–59. <https://doi.org/10.1007/s11104-008-9833-8>
- 661

- 662 Gaby JC, Buckley DH (2012) A comprehensive evaluation of PCR primers to amplify the *nifH* gene of
663 nitrogenase. *PLoS ONE*, 7(7), e42149. <https://doi.org/10.1371/journal.pone.0042149>
- 664 Ghodhbane-Gtari F, Nouioui I, Hezbri K, Lundstedt E, D'Angelo T, McNutt Z, Laplaze L, Gherbi H, Vaissayre
665 V, Svistoonoff S, ben Ahmed H, Boudabous A, Tisa LS (2019) The plant-growth-promoting
666 actinobacteria of the genus *Nocardia* induces root nodule formation in *Casuarina glauca*. *Antonie van*
667 *Leeuwenhoek*, 112, 75–90. <https://doi.org/10.1007/s10482-018-1147-0>
- 668 Goldman JC, Caron DA, Dennett MR (1987) Regulation of gross growth efficiency and ammonium
669 regeneration in bacteria by substrate C: N ratio. *Limnol. Oceanogr.*, 32(6), 1239–1252.
670 <https://doi.org/10.4319/lo.1987.32.6.1239>
- 671 Hardy RWF, Burns RC, Holsten RD (1973) Applications of the acetylene-ethylene assay for measurement
672 of nitrogen fixation. *Soil Biol. Biochem.*, 5(1), 47–81. [https://doi.org/10.1016/0038-0717\(73\)90093-X](https://doi.org/10.1016/0038-0717(73)90093-X)
- 673 Heldal M, Norland S, Tumyr O (1985). X-ray microanalytic method for measurement of dry matter and
674 elemental content of individual bacteria. *Appl. Environ. Microbiol.*, 50(5), 1251–1257.
675 <https://doi.org/10.1128/aem.50.5.1251-1257.1985>
- 676 Heuck C, Weig A, Spohn M (2015) Soil microbial biomass C:N:P stoichiometry and microbial use of organic
677 phosphorus. *Soil Biol. Biochem.*, 85, 119–129. <https://doi.org/10.1016/j.soilbio.2015.02.029>
- 678 Hu J, Tang H, Wang YZ, Yang C, Gao M, Tsang YF, Li J (2022) Effect of dissolved solids released from
679 biochar on soil microbial metabolism. *Environ. Sci.: Processes Impacts*, 24, 598–608.
680 <https://doi.org/10.1039/D2EM00036A>
- 681 Hu X, Kerckhof FM, Ghesquière J, Bernaerts K, Boeckx P, Clauwaert P, Boon N (2020) Microbial protein
682 out of thin air: fixation of nitrogen gas by an autotrophic hydrogen-oxidizing bacterial enrichment.
683 *Environ. Sci. Technol.*, 54(6), 3609–3617. <https://doi.org/10.1021/acs.est.9b06755>
- 684 Huang X, Liu L, Zhao J, Zhang J, Cai Z (2019) The families *Ruminococcaceae*, *Lachnospiraceae*, and
685 *Clostridiaceae* are the dominant bacterial groups during reductive soil disinfection with
686 incorporated plant residues. *Appl. Soil Ecol.*, 135, 65–72. <https://doi.org/10.1016/j.apsoil.2018.11.011>
- 687 Huda N u, Tanvir R, Badar J, Ali I, Rehman Y (2022) Arsenic-resistant plant growth promoting
688 *Pseudoxanthomonas mexicana* S254 and *Stenotrophomonas maltophilia* S255 isolated from
689 agriculture soil contaminated by industrial effluent. *Sustainability*, 14(17), 10697.
690 <https://doi.org/10.3390/su141710697>
- 691 Kandemir T, Schuster ME, Senyshyn A, Behrens M, Schlögl R (2013) The Haber–Bosch process revisited:
692 on the real structure and stability of “ammonia iron” under working conditions. *Angew. Chem., Int.*
693 *Ed. Engl.*, 52(48), 12723–12726. <https://doi.org/10.1002/anie.201305812>
- 694 Khan KS, Mack R, Castillo X, Kaiser M, Joergensen RG (2016) Microbial biomass, fungal and bacterial
695 residues, and their relationships to the soil organic matter C/N/P/S ratios. *Geoderma*, 271, 115–123.
696 <https://doi.org/10.1016/j.geoderma.2016.02.019>
- 697 Kifle MH, Laing MD (2016) Isolation and screening of bacteria for their diazotrophic potential and their
698 influence on growth promotion of maize seedlings in greenhouses. *Front. Plant Sci.*, 6, 1225.
699 <https://doi.org/10.3389/fpls.2015.01225>
- 700 Kim J, Rees DC (1994) Nitrogenase and biological nitrogen fixation. *Biochemistry*, 33, 389–397.
701 <https://doi.org/10.1021/bi00168a001>
- 702 Klemps R, Cypionka H, Widdel F, Pfennig N (1985) Growth with hydrogen, and further physiological
703 characteristics of *Desulfotomaculum* species. *Arch. Microbiol.*, 143, 203–208.
704 <https://doi.org/10.1007/BF00411048>
- 705 Lin L, Li Z, Hu C, Zhang X, Chang S, Yang L, Li Y, An Q (2012) Plant growth-promoting nitrogen-fixing
706 enterobacteria are in association with sugarcane plants growing in Guangxi, China. *Microbes Environ.*,
707 27(4), 391–398. <https://doi.org/10.1264/jsme2.me11275>
- 708 Liu A, Yang Y, Ren X, Zhao Q, Gao M, Guan W, Meng F, Gao L, Yang Q, Liang X, Ma T (2020) Current
709 progress of electrocatalysts for ammonia synthesis through electrochemical nitrogen reduction under
710 ambient conditions. *ChemSusChem*, 13(15), 3766–3788. <https://doi.org/10.1002/cssc.202000487>
- 711 Liu C, Sakimoto KK, Colón BC, Silver PA, Nocera DG (2017) Ambient nitrogen reduction cycle using a
712 hybrid inorganic–biological system. *Proc. Natl. Acad. Sci.*, 114(25), 6450–6455.
713 <https://doi.org/10.1073/pnas.1706371114>

- 714 Liu F, Zhao C, Xia L, Yang F, Chang X, Wang Y (2011) Biofouling characteristics and identification of
715 preponderant bacteria at different nutrient levels in batch tests of a recirculating cooling water
716 system. *Environ. Technol.*, 32(8), 901–910. <https://doi.org/10.1080/09593330.2010.517220>
- 717 Loferer-Krößbacher M, Klima J, Psenner R. (1998) Determination of bacterial cell dry mass by
718 transmission electron microscopy and densitometric image analysis. *Appl. Environ. Microbiol.*, 64(2),
719 688–694. <https://doi.org/10.1128/AEM.64.2.688-694.1998>
- 720 Logan BE, Rossi R, Ragab A, Saikaly PE (2019) Electroactive microorganisms in bioelectrochemical
721 systems. *Nat. Rev. Microbiol.*, 17, 307-319. <https://doi.org/10.1038/s41579-019-0173-x>
- 722 Martín A J, Shinagawa T, Pérez-Ramírez J. (2019) Electrocatalytic reduction of nitrogen: from Haber-Bosch
723 to ammonia artificial leaf. *Chem*, 5(2), 263-283. <https://doi.org/10.1016/j.chempr.2018.10.010>
- 724 Masclaux-Daubresse C, Daniel-Vedele F, Dechorgnat J, Chardon F, Gaufichon L, Suzuki A. (2010) Nitrogen
725 uptake, assimilation and remobilization in plants: Challenges for sustainable and productive
726 agriculture. *Ann. Bot.*, 105(7), 1141–1157. <https://doi.org/10.1093/aob/mcq028>
- 727 McMurdie PJ (2023) *Phyloseq* [R]. <https://github.com/joey711/phyloseq> (Original work published 2011)
- 728 Minamisawa K, Nishioka K, Miyaki T, Ye B, Miyamoto T, You M, Saito A, Saito M, Barraquio WL,
729 Teaumroong N, Sein T, Sato T (2004) Anaerobic nitrogen-fixing consortia consisting of *Clostridia*
730 isolated from gramineous plants. *Appl. Environ. Microbiol.*, 70(5), 3096-3102.
731 <https://doi.org/10.1128/AEM.70.5.3096-3102.2004>
- 732 Moreno-Vivián C, Caballero FJ, Cárdenas J, Castillo F (1989) Effect of the C/N balance on the regulation of
733 nitrogen fixation in *Rhodobacter capsulatus* E1F1. *Biochim. Biophys. Acta Bioenerg.*, 977(3), 297–300.
734 [https://doi.org/10.1016/S0005-2728\(89\)80083-0](https://doi.org/10.1016/S0005-2728(89)80083-0)
- 735 Moscoviz R, Desmond-Le Quéméner E, Trably E, Bernet N (2019) Bioelectrochemical Systems for the
736 Valorization of Organic Residues. In J.-R. Bastidas-Oyanedel & J. E. Schmidt (Eds.), *Biorefinery:
737 Integrated Sustainable Processes for Biomass Conversion to Biomaterials, Biofuels, and Fertilizers* (pp.
738 511–534). Springer International Publishing. https://doi.org/10.1007/978-3-030-10961-5_21
- 739 Paul D, Noori MT, Rajesh PP, Ghangrekar MM, Mitra A (2018) Modification of carbon felt anode with
740 graphene oxide-zeolite composite for enhancing the performance of microbial fuel cell. *Sustain.
741 Energy Technol. Assess.*, 26, 77–82. <https://doi.org/10.1016/j.seta.2017.10.001>
- 742 Peoples MB, Craswell ET (1992) Biological nitrogen fixation: Investments, expectations and actual
743 contributions to agriculture. *Plant Soil*, 141(1), 13–39. <https://doi.org/10.1007/BF00011308>
- 744 Pogoreutz C, Rådecker N, Cárdenas A, Gärdes A, Wild C, Voolstra CR (2017) Nitrogen fixation aligns with
745 *nifH* abundance and expression in two coral trophic functional groups. *Front. Microbiol.*, 8.
746 <https://www.frontiersin.org/articles/10.3389/fmicb.2017.01187>
- 747 Poly F, Ranjard L, Nazaret S, Gourbière F, Monrozier L J (2001) Comparison of *nifH* gene pools in soils and
748 soil microenvironments with contrasting properties. *Appl. Environ. Microbiol.*, 67(5), 2255–2262.
749 <https://doi.org/10.1128/AEM.67.5.2255-2262.2001>
- 750 Postgate JR (1970) Nitrogen fixation by sporulating sulphate-reducing bacteria including rumen strains. *J.
751 Gen. Microbiol.*, 63(1), 137–139. <https://doi.org/10.1099/00221287-63-1-137>
- 752 Rago L, Zecchin S, Villa F, Goglio A, Corsini A, Cavalca L, Schievano A (2019) Bioelectrochemical nitrogen
753 fixation (e-BNF): electro-stimulation of enriched biofilm communities drives autotrophic nitrogen and
754 carbon fixation. *Bioelectrochem.*, 125, 105–115. <https://doi.org/10.1016/j.bioelechem.2018.10.002>
- 755 Rojas-Tapias D, Moreno-Galván A, Pardo-Díaz S, Obando M, Rivera D, Bonilla R (2012) Effect of
756 inoculation with plant growth-promoting bacteria (PGPB) on amelioration of saline stress in maize
757 (*Zea mays*). *Appl. Soil Ecol.*, 61, 264–272. <https://doi.org/10.1016/j.apsoil.2012.01.006>
- 758 Rous, A. (2023). *Script and data used for the article 'Comparison of enrichment methods for efficient
759 nitrogen fixation on a biocathode'* (V1 ed.). Recherche Data Gov. <https://doi.org/10.57745/ONNGWZ>
- 760 Ryan RP, Monchy S, Cardinale M, Taghavi S, Crossman L, Avison MB, Berg G, van der Lelie D, Dow JM
761 (2009) The versatility and adaptation of bacteria from the genus *Stenotrophomonas*. *Nature Reviews
762 Microbiology*, 7, 5114-525. <https://doi.org/10.1038/nrmicro2163>
- 763 Saiz E, Sgouridis F, Drijfhout FP, Ullah S (2019) Biological nitrogen fixation in peatlands: Comparison
764 between acetylene reduction assay and ¹⁵N₂ assimilation methods. *Soil Biol. Biochem.*, 131, 157–165.
765 <https://doi.org/10.1016/j.soilbio.2019.01.011>
- 766 Singh RK, Singh P, Li HB, Guo DJ, Song QQ, Yang T, Malviya MK, Song XP, Li YR. (n.d.). Plant-PGPR
767 interaction study of plant growth-promoting diazotrophs *Kosakonia radicincitans* BA1

- 768 and *Stenotrophomonas maltophilia* COA2 to enhance growth and stress-related gene expression
769 in *Saccharum* spp. *J. Plant Interact.*, 15(1), 427-445. <https://doi.org/10.1080/17429145.2020.1857857>
- 770 Soper FM, Simon C, Jauss V (2021) Measuring nitrogen fixation by the acetylene reduction assay (ARA): Is
771 3 the magic ratio? *Biogeochemistry*, 152(2), 345–351. <https://doi.org/10.1007/s10533-021-00761-3>
- 772 Stoddard SF, Smith BJ, Hein R, Roller BRK, Schmidt TM (2015) *rrnDB*: Improved tools for interpreting rRNA
773 gene abundance in bacteria and archaea and a new foundation for future development. *Nucleic Acids*
774 *Res.*, 43(D1), D593–D598. <https://doi.org/10.1093/nar/gku1201>
- 775 Temple SJ, Vance CP, Stephen Gantt J (1998) Glutamate synthase and nitrogen assimilation. *Trends Plant*
776 *Sci.*, 3(2), 51–56. [https://doi.org/10.1016/S1360-1385\(97\)01159-X](https://doi.org/10.1016/S1360-1385(97)01159-X)
- 777 *Tidyverse*. (n.d.). Retrieved 9 February 2023, from <https://www.tidyverse.org/>
- 778 Tilak KVBR, Schneider K, Schlegel HG (1986) Autotrophic growth of nitrogen-fixing *Azospirillum* species
779 and partial characterization of hydrogenase from strain CC. *Current Microbiol.*, 13(6), 291–297.
780 <https://doi.org/10.1007/BF01577194>
- 781 Wiegel J (2006). The Genus *Xanthobacter*. In: Dworkin, M., Falkow, S., Rosenberg, E., Schleifer, KH.,
782 Stackebrandt, E. (eds) *The Prokaryotes*. Springer, New York, NY. [https://doi.org/10.1007/0-387-](https://doi.org/10.1007/0-387-30745-1_16)
783 [30745-1_16](https://doi.org/10.1007/0-387-30745-1_16)
- 784 Wresta A, Widyarani R, Boopathy R, Setiadi T (2021) Thermodynamic approach to estimating reactions
785 and stoichiometric coefficients of anaerobic glucose and hydrogen utilization. *Eng. Rep.*, 3(6), e12347.
786 <https://doi.org/10.1002/eng2.12347>
- 787 Wu Y, Zaiden N, Cao B (2018) The core- and pan-genomic analyses of the genus *Comamonas*: from
788 environmental adaptation to potential virulence. *Front. Microbiol.*, 9, 3096.
789 <https://doi.org/10.3389/fmicb.2018.03096>
- 790 Hafeez FY, Yasmin S, Ariani D, Rahman Mu, Zafar Y, Malik KA (2006). Plant growth-promoting bacteria as
791 biofertilizer. *Agron. Sustain. Dev.*, 26(2), 143–150. <https://doi.org/10.1051/agro:2006007>
- 792 Yadav R, Chiranjeevi P, Yadav S, Singh R, Patil, SA (2022) Electricity-driven bioproduction from CO₂ and N₂
793 feedstocks using enriched mixed microbial culture. *J. CO₂ Util.*, 60, 101997.
794 <https://doi.org/10.1016/j.jcou.2022.101997>
- 795 Yaghoubi Khanghahi M, Strafella S, Allegretta I, Crecchio C (2021) Isolation of bacteria with potential
796 plant-promoting traits and optimization of their growth conditions. *Current Microbiol.*, 78(2), 464–
797 478. <https://doi.org/10.1007/s00284-020-02303-w>
- 798 Zaybak Z, Pisciotta JM, Tokash JC, Logan BE (2013) Enhanced start-up of anaerobic facultatively
799 autotrophic biocathodes in bioelectrochemical systems. *J. Biotechnol.*, 168(4), 478–485.
800 <https://doi.org/10.1016/j.jbiotec.2013.10.001>
- 801 Zhang L, Tian C, Wang H, Gu W, Zheng D, Cui M, Wang X, He X, Zhan G, Li D (2022). Improving
802 electroautotrophic ammonium production from nitrogen gas by simultaneous carbon dioxide fixation
803 in a dual-chamber microbial electrolysis cell. *Bioelectrochem.*, 144, 108044.
804 <https://doi.org/10.1016/j.bioelechem.2021.108044>
- 805 Zhang W, Yu C, Wang X, Hai L (2020) Increased abundance of nitrogen transforming bacteria by higher
806 C/N ratio reduces the total losses of N and C in chicken manure and corn stover mix composting.
807 *Biores. Technol.*, 297, 122410. <https://doi.org/10.1016/j.biortech.2019.122410>
- 808 Zhang Y, Hu T, Wang H, Jin H, Liu Q, Chen Z, Xie Z (2022). Nitrogen content and C/N ratio in straw are the
809 key to affect biological nitrogen fixation in a paddy field. *Plant Soil*, 481, 535-546.
810 <https://doi.org/10.1007/s11104-022-05654-4>